

# STRUCTURE AND FEEDBACK STABILIZATION OF RESISTIVE WALL MODES IN DIII-D

L.C. Johnson,<sup>1</sup> M. Okabayashi,<sup>1</sup> A.M. Garofalo,<sup>2</sup> E.J. Strait,<sup>3</sup> J. Bialek,<sup>2</sup>  
M.S. Chance,<sup>1</sup> M.S. Chu,<sup>3</sup> E.D. Fredrickson,<sup>1</sup> R.J. La Haye,<sup>3</sup> J. Manickam,<sup>1</sup>  
A. Nagy,<sup>1</sup> G.A. Navratil,<sup>2</sup> R.T. Snider,<sup>3</sup> J.T. Scoville,<sup>3</sup> A.D. Turnbull,<sup>3</sup>  
and M.L. Walker<sup>3</sup>

<sup>1</sup>Princeton Plasma Physics Laboratory, Princeton, New Jersey

<sup>2</sup>Columbia University, New York, New York

<sup>3</sup>General Atomics, San Diego, California

## Abstract

Under normal circumstances, the resistive wall mode (RWM) limits the performance of discharges in the DIII-D tokamak when the plasma beta exceeds the no-wall ideal stability limit. These  $n=1$  global kink modes grow on the slow time scale of magnetic diffusion through the surrounding conductive vacuum vessel wall. Active magnetic feedback stabilization experiments on DIII-D during the 2000 campaign succeeded in suppressing the resistive wall mode for periods more than fifty times longer than the resistive penetration time of the wall. Experiments in 2001 have demonstrated dramatic improvements in active control capability, owing largely to an extensive new set of magnetic sensors installed inside the vacuum vessel after the 2000 campaign. The new internal magnetic sensors, together with pre-existing external sensors and a toroidal array of x-ray cameras, have also afforded better characterization of the previously observed mode structure.

## 1. The Feedback System

Substantial progress was made in active magnetic feedback stabilization of resistive wall modes in DIII-D during the 2000 experimental campaign [1-4]. Control capability was significantly improved before the 2001 campaign by the addition of new sets of magnetic sensors inside the vacuum vessel. The locations of the magnetic sensors and active coils now in use for feedback stabilization experiments on DIII-D are illustrated in Fig. 1. Radial magnetic field perturbations  $\delta B_r$  arising from growth of RWMs are detected by diametrically opposed pairs of large-area saddle loops. Six external loops and six internal loops, each covering a  $60^\circ$  toroidal arc, are arranged along the vessel midplane, outboard of the plasma.  $\delta B_r$  mode detection is augmented by two additional 12-loop toroidal arrays of external sensors and two six-loop arrays of internal sensors situated above and below the midplane arrays. Poloidal

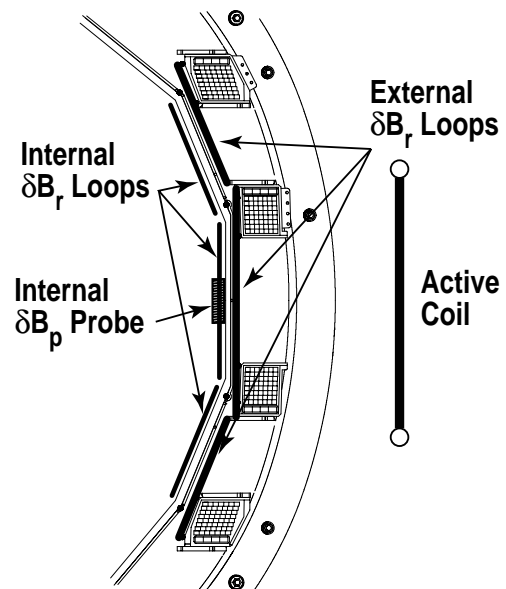


Fig. 1. Locations of RWM sensors and active coils on DIII-D.

magnetic field perturbations  $\delta B_p$  are detected by four diametrically opposed pairs of internal magnetic probes. The measurements are used to generate commands for applying power to three pairs of picture frame active coils located outside the tokamak field coils at the same toroidal locations as the midplane saddle loops. The most commonly used feedback logic algorithms are the “smart shell” scheme, where the net radial flux through the saddle loops is nulled, and the “explicit mode control” scheme, where the feedback system attempts to suppress the residual flux from the mode after subtracting contributions from the active coils [3].

## 2. Structure of Resistive Wall Modes

External  $\delta B_r$  sensors were used for the first measurements of the helical structure of RWMs in DIII-D [3]. All three toroidal arrays of external saddle loops showed similar but phase shifted behavior, corresponding to a poloidal mode number in the range of 2 to 3. Recent measurements with internal saddle loops are essentially the same. This kind of helical structure is in agreement with expectations [5,6] and has been observed in all experiments so far, both with and without closed-loop feedback.

Soft x-ray data from two toroidally separated but otherwise identical poloidal arrays can be used to measure the relative radial plasma displacement between the two locations. Figure 2(a) shows x-ray intensities along six poloidal sight lines from cameras at toroidal locations of  $45^\circ$  and  $195^\circ$ , respectively, for a feedback stabilized plasma. In this case, the “smart shell” feedback algorithm was used with the internal midplane saddle loops. The x-ray data show an asymmetry beginning at about 1420 ms, although the feedback system manages to delay the final beta collapse until 1540 ms. Figure 2(b) shows the amplitudes of  $\delta B_r$  and  $\delta B_p$  as determined by the external midplane loops and the magnetic probes, respectively. A scaling factor of 2 is applied to the  $\delta B_r$  data to compensate for spatial smoothing by the large-area saddle loops. Chord-by-chord comparisons of the x-ray data can be used to find the relative radial displacements between the two toroidal locations at minor radii corresponding

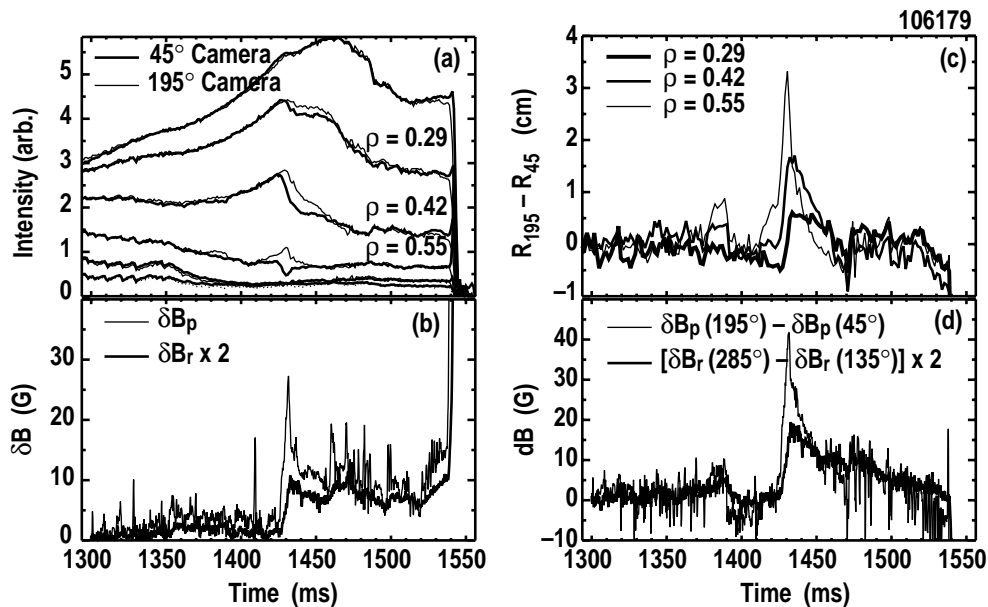


Fig. 2. Soft x-ray and magnetic sensor data for a feedback stabilized plasma. Relative radial displacements of the plasma ( $R_{195} - R_{45}$ ) between two toroidally separated soft x-ray cameras are in good agreement with corresponding differences in magnetic perturbations.

to the x-ray sight lines. Relative displacements ( $R_{195}$ – $R_{45}$ ) for three values of the minor radius  $\rho$  are shown in Fig. 2(c). For comparison, Fig. 2(d) shows the differences in  $\delta B_p$  and  $\delta B_r$  between corresponding toroidal locations, as deduced from the amplitudes and phases of the magnetic measurements and taking into account the  $90^\circ$  toroidal phase shift between poloidal and radial perturbations. The time behavior of the curves in Fig. 2(d) differs from that of the mode amplitudes shown in Fig. 2(b) because of mode rotation relative to the fixed camera positions. Although both the x-ray measurements of relative radial displacements and the magnetic measurements of relative field perturbations indicate a time varying internal structure of the mode, the results are consistent with a global kink and are generally in agreement with previous observations and theoretical predictions [3,5,6].

### 3. Closed-Loop Feedback Stabilization Using Internal Magnetic Sensors

Closed-loop feedback stabilization experiments on DIII-D prior to the installation of internal sensors derived error signals from the midplane external saddle loops and used either “smart shell” or “explicit mode control” feedback logic. Simulations of feedback stabilization of resistive wall modes in DIII-D have been carried out for a variety of assumed hardware configurations, using the VALEN code and “smart shell” logic [3,7]. The modeling predicts that properly designed internal  $\delta B_r$  sensors will enable significantly greater control capability than that possible with existing external saddle loops and that internal  $\delta B_p$  sensors will offer even greater advantages because of their insensitivity to radial fields from the active coils.

Recent experiments using the new internal sensors confirm these predictions.

Figure 3(a) shows toroidal plasma rotation data for discharges where a rapid plasma current ramp was used to reliably trigger an RWM at about 1400 ms in the absence of feedback stabilization [2]. Toroidal rotation is a sensitive indicator of the presence of an RWM, since even a small amplitude mode produces a significant drag on the rotation. Using the “smart shell” feedback algorithm, internal saddle loops were more effective than external loops in extending the plasma duration. Figure 3(b) compares results for a plasma condition with slightly lower initial rotation frequency. Using the  $\delta B_p$  sensors and the “explicit mode control” algorithm, the increase in plasma duration was almost five times as long as that achieved using the internal saddle loops and the “smart shell” algorithm.

Figure 4 shows data for a case with slow plasma current ramp and  $\delta B_p$  feedback where the discharge was sustained for almost a second at pressures approaching twice the no-wall stability limit. The toroidal rotation frequency is essentially constant until the end of the discharge. In another discharge from the same series, the active coil currents were pre-programmed open-loop to match the slowly varying behavior of currents arising from closed-

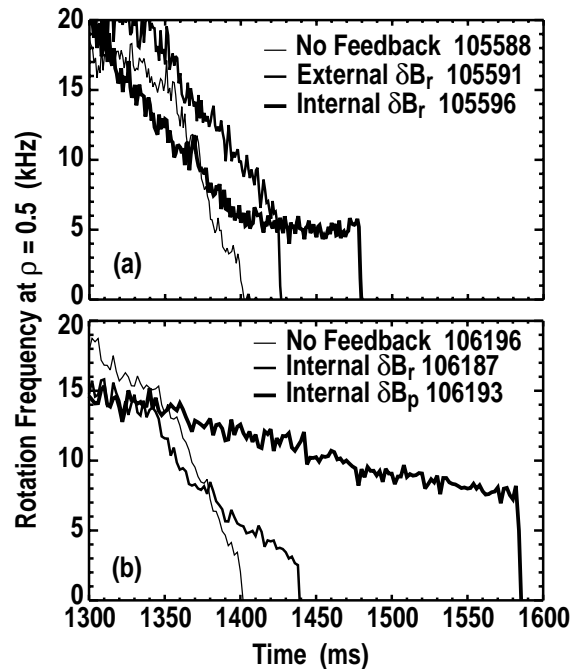


Fig. 3. Comparisons of stabilized plasma duration for a variety of feedback conditions.

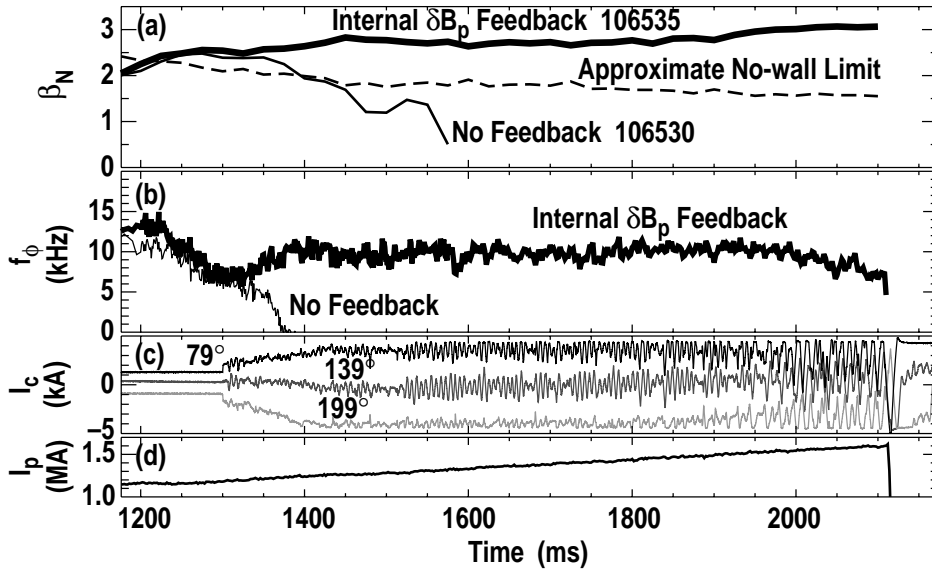


Fig. 4. (a)  $\beta_N$ , (b) toroidal rotation frequency at  $\rho=0.5$ , (c) currents in the three pairs of active coils, and (d) plasma current for shot 106535 with internal  $\delta B_p$  feedback. For comparison,  $\beta_N$  and rotation frequency are also shown for shot 106530 without feedback.

looped  $\delta B_p$  feedback in the previous discharge. The pressures and rotation frequencies for the two shots were essentially the same and similar in value to those shown in Fig. 4. In this case, closed-loop  $\delta B_p$  feedback provides dynamic correction of magnetic error fields, reducing their braking effect on the rotation. The resulting sustained toroidal rotation enhances the stabilizing effect of the conductive wall. Detailed analysis is in progress [8].

#### 4. Summary

Extensive new arrays of internal magnetic sensors, together with external sensors and toroidally distributed soft x-ray cameras, have been used to confirm the previously observed and theoretically predicted global kink nature of resistive wall modes. Closed-loop feedback stabilization experiments using the internal sensors support predicted improvements in mode control with respect to previously reported results using external sensors. With active control, plasmas have been sustained for almost a second at pressures approaching twice the no-wall limit.

#### Acknowledgment

Work supported by U.S. Department of Energy under Contacts DE-AC02-76CH03073 and DE-AC03-99ER54463 and Grants DE-FG02-89ER53297 and DE-FG03-95ER54309.

#### References

- [1] Strait, E.J., *et al.*, Phys. Rev. Lett. **74**, 2483 (1995).
- [2] Garofalo, A.M., *et al.*, Phys. Rev. Lett. **82**, 3811 (1999).
- [3] Okabayashi, M., *et al.*, Phys. Plasmas **8**, 2071 (2001).
- [4] Garofalo, A.M., *et al.*, Nucl. Fusion **40**, 1491 (2000).
- [5] Chance, M., *et al.*, submitted to Nucl. Fusion.
- [6] Turnbull, A.D., *et al.*, submitted to Nucl. Fusion.
- [7] Bialek, J., *et al.*, Phys. Plasmas **8**, 2170 (2001).
- [8] Garofalo, A.M., *et al.*, to be published.